JOURNAL OF SPACECRAFT AND ROCKETS
Vol. 40, No. 5, September–October 2003

Response of a Near Spherically Symmetric Spacecraft to a Stuck-On Thruster

Trevor Williams*
University of Cincinnati, Cincinnati, Ohio 45221
and
Sergei Tanygin†
Analytical Graphics, Inc., Malvern, Pennsylvania 19355

If a spacecraft experiences a stuck-on thruster that does not act through its center of mass, it can experience significant attitude and translational motions. These motions are analyzed for the case of a vehicle that is nearly spherically symmetric; any real spacecraft that is designed to be perfectly symmetric will actually be near symmetric in practice, as a result of small irregularities in its mass distribution. It is shown that the motion that such a vehicle experiences as a result of a prolonged thruster firing is significantly more complicated than the simple spin that is obtained for the ideal spherical case. In particular, the real spacecraft will experience a form of forced nutation, with convergence toward either its major or minor principal axis, depending on both the applied torque and the mass properties of the vehicle. Furthermore, the principal axis that is converged to generally will not be orthogonal to the thruster axis. Consequently, the thrust vector may have a significant component along the converged spin axis, thus, giving rise to a considerable net linear acceleration on the vehicle. The large Δv that can result is fundamentally different from the behavior in the ideal perfect sphere case and will occur, to varying extents, for virtually all near-symmetric mass properties. Methods are derived for predicting this Δv and other aspects of the stuck-on thruster behavior of near-symmetric vehicles, for any given set of mass properties, and the new analytical results are fully illustrated by means of numerical simulations.

Nomenclature

a	=	linear acceleration, m/s^2
f	=	force applied by stuck-on thruster, N
I_0	=	nominal axial moment inertia of spacecraft, kg · m^2
m	=	mass of spacecraft, kg
$R(\tau)$	=	torque Rayleigh quotient, kg · m^2
r	=	radius of spherical spacecraft, m
t_{45}, t_{trans}, t_{asymp}	=	time constants of spacecraft response to stuck-on thruster, s
$\bar{\boldsymbol{x}}$	=	offset of center of mass from geometric center of thrusters, m
α	=	angular acceleration, rad/s^2
ΔI	=	inertia matrix perturbation, kg · m^2
Δv	=	translational speed imparted by thruster, m/s
θ	=	angle between vectors $\hat{\boldsymbol{\omega}}$ and $\hat{\boldsymbol{\tau}}$, rad
λ_1, λ_2	=	perturbations in principal moments of inertia, kg · m^2
$\tilde{\lambda}_1$, $\tilde{\lambda}_2$	=	normalized principal moment perturbations
$\boldsymbol{\tau}$	=	thruster torque vector about center of mass in body coordinates, N · m
$\hat{\boldsymbol{\tau}}$	=	thruster torque vector in principal coordinates (with components $\{\hat{\tau}_i\}$), N · m
$\boldsymbol{\omega}$	=	angular velocity vector of spacecraft in body coordinates, rad/s
$\hat{\boldsymbol{\omega}}$	=	angular velocity vector in principal coordinates (with components $\{\hat{\omega}_i\}$), rad/s

Received 26 October 2000; revision received 3 March 2003; accepted for publication 3 March 2003.

*Professor, Department of Aerospace Engineering; Trevor.Williams@uc.edu. Associate Fellow AIAA.
†Senior Astro-Development Engineer, 325 Technology Drive; stanygin@stk.com.

Introduction

IF a spacecraft experiences a stuck-on thruster that does not act through its center of mass, it will be excited by a body-fixed force and torque and, consequently, can experience significant attitude and translational motion. The serious consequences that can result from this type of event are illustrated by the following three examples: the Gemini 8 manned spacecraft[1] in 1966, the Clementine lunar/asteroid probe,[2] and the Wide-Field Infrared Explorer (WIRE) infrared astronomy satellite. The Gemini 8 mission had to be truncated from the planned 3 days to just 10 h, with the crew performing an emergency reentry at the earliest possible opportunity, after a yaw thruster became stuck-on. Clementine was lost after a software problem led to its thrusters firing until propellant depletion, causing the spacecraft to reach a spin rate of over 80 rpm; the intended asteroid flyby could not be performed. More recently, the WIRE spacecraft was prevented from carrying out any of its planned mission by the inadvertent venting of its on-board cryogen supply shortly after launch in 1999. This venting event was dynamically similar to a stuck-on thruster and led to very high spacecraft rotation rates.

Several important dynamic questions arise in connection with the stuck-on thruster problem and will be addressed in this paper. First, how do the spacecraft rotational rates build up with time and along which axes? Second, how does the orientation of the body-fixed thruster evolve? These answers will in turn determine the answer to a third question: To what extent does the applied thrust gives rise to a net linear acceleration? If a significant acceleration is produced, the resulting Δv can have important safety implications: For instance, the orbit of the spacecraft may be perturbed significantly and, if it is flying in proximity with another vehicle, a collision may result. A final question is as follows. What is the asymptotic rotational acceleration of the vehicle? This value will determine how long the spacecraft will take to reach any specified rotation rate, for instance, its structural integrity limit.

Certain of these questions have been addressed in the literature for various special cases, namely, that of an axisymmetric vehicle,[3,4] one that is nearly so,[5,6] or a general spacecraft with torque constrained

Table 1 AERCam Sprint dynamics parameters

Parameter	Value
Mass fully fueled	15.8 kg (34.9 lbm)
Propellant mass	0.28 kg (0.62 lbm)
Vehicle radius	0.178 m (7.0 in.)
Mean axial moment of inertia	0.160 kg · m^2 (547 lbm $in.^2$)
Thrust per jet	0.38 N (0.085 lbf)
Thruster moment arms	0.102 m (4.0 in.)
One-jet linear acceleration	0.024 m/s^2 (0.08 ft/s^2)
Mean one-jet angular acceleration	0.241 rad/s^2 (13.8 deg/s^2)

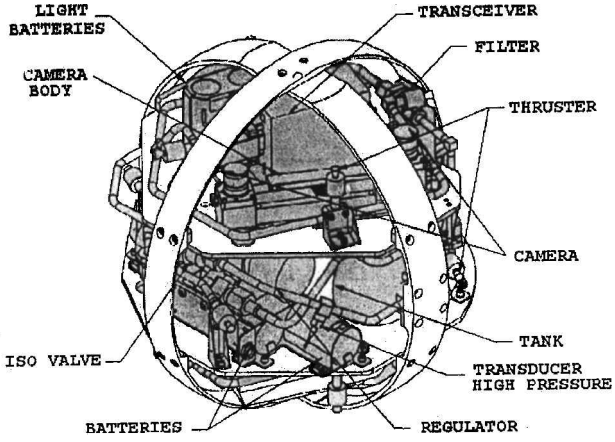

Fig. 1 AERCam Sprint general layout.

to lie along one of its principal axes.[3,7] However, the application that motivates the present work and that leads to the new results that are derived here is not covered by any of the existing analyses. This is the case of a spacecraft that is nominally spherically symmetric, but actually (as is inevitable in practice) has mass properties that are slightly perturbed from the spherical case and that is excited by a tangential thruster that produces a torque that is not parallel to any of the principal axes of the body. This problem, which is of considerable theoretical interest, is also of significant practical interest: it is motivated by safety analyses performed in connection with the Autonomous Extra Vehicular Activity (EVA) Robotic Camera (AERCam) Sprint vehicle[8] that was developed by NASA Johnson Space Center. Sprint (Fig. 1) is a small, spherical, remotely piloted "camera pod," with 12 tangential nitrogen thrusters providing full six-degree-of-freedom control; its key dynamic parameters are given in Table 1. This spacecraft is a prototype of a device to permit inspection of the exterior of the International Space Station without requiring the involvement of EVA astronauts. (Such a device would have been very useful on the Mir station after its collision with the Progress cargo spacecraft in June 1997.) Sprint was test flown in close proximity to Space Shuttle *Columbia* during the STS-87 mission in December 1997 (Fig. 2). Clearly, it is important to have a full understanding of the dynamics of a stuck-on thruster event, and its possible safety implications when considering a spacecraft that is performing orbital proximity operations with a crewed vehicle.

In this paper, we first briefly address the motion that would be obtained for a stuck-on thruster on an ideal, perfectly spherical vehicle. This behavior is very simple and not of great interest in itself, but provides a useful baseline for comparison with what is found in the more realistic near-symmetric case. (Note that the term near symmetric is used here to denote a body that is nearly spherically symmetric, with all moments of inertia approximately equal. By contrast, the same term was previously used in Refs. 5 and 6 to denote a body that is nearly axisymmetric, with two moments approximately equal and the third distinct.) For the ideal body, the axis of rotation of the induced motion is simply along the applied torque direction. As a result, the applied force cancels as the vehicle rotates: The only net Δv results from the very first phase of the motion,[9] before a significant rotation rate has been set up. With this as background, the near-symmetric case is studied. It is shown that the motion caused by a stuck-on thruster on such a vehicle

Fig. 2 AERCam Sprint during on-orbit test flight.

is fundamentally different from that which applies for the perfect sphere. In fact, the response is shown to now break down into three distinct phases: an initial phase, where the motion is much as in the ideal case; a transition phase, with rather complicated body rates; and an asymptotic phase, where the motion approaches a spin about either the major or minor principal axis of the spacecraft. Furthermore, the durations of these phases are shown to be functions of the mass properties of the vehicle and the angular acceleration produced by the stuck-on thruster.

The fundamental stuck-on thruster dynamics questions that were stated initially are then all answered for the near-spherical spacecraft. In particular, a method is given for determining which applied thrust directions will cause migration to a major axis spin and which to a minor, and the associated asymptotic angular acceleration is characterized. Also, a physical description of the resulting forced nutation behavior is provided, and a relationship is given for determining the time-varying frequency of this nutation. Finally, the resulting net linear acceleration in the asymptotic phase of the motion is derived also. Because the principal axes of a near-spherical body can be rotated through large angles by small mass distribution irregularities, it will be shown that it is possible for the spin to converge to a principal axis that makes only a small angle to the applied thrust vector. Consequently, the asymptotic linear acceleration can approach the one jet thrust/mass ratio of the spacecraft for the worst possible combination of thrust direction and vehicle mass properties. Furthermore, this acceleration can act for an extended period of time, unlike the short initial period that produces a Δv in the ideal case. The Δv resulting from a stuck-on thruster on a realistic, near-spherical vehicle may, therefore, be very much greater than that obtained for an ideal symmetric one. In fact, it will be shown that virtually all near-symmetric mass properties will give rise to a significant Δv in response to a long-duration stuck-on thruster; different mass properties differ only in degrees, that is, in the precise value of the asymptotic acceleration and the time it takes to become established. The analytical expressions that are derived for these quantities, and the others that describe the response of a near-symmetric vehicle to a stuck-on thruster, will be illustrated in detail by means of numerical simulation results.

Stuck-On Thruster, Spherically Symmetric Case

We shall first briefly consider an idealized problem where the vehicle is perfectly spherically symmetric. The results obtained for this case are quite simple and serve as a baseline for the much more complicated conclusions reached for the more realistic near-symmetric case. Of course, the major effect of a single stuck-on

thruster in the symmetric case is to spin up the vehicle about the applied torque axis. Consequently, the linear acceleration that is applied by the firing jet cancels over the course of each revolution of the vehicle. Therefore, it might be concluded that no net Δv results from a stuck-on thruster in this case. However, this conclusion is only approximately accurate. The reason is that the applied thrust acts in a nearly constant direction during the initial phase of the motion, when the vehicle still has low rotation rates. The linear acceleration during this early period, therefore, does not cancel, thus, giving rise to a nonzero net Δv. This Δv magnitude, and the time taken for it to develop, will now be characterized.

For definiteness, the spherically symmetric spacecraft will be assumed to be equipped with 12 tangential jets of thrust f and moment arm r. These are arranged as in the AERCam Sprint design, that is, two thrusters are parallel to the $+x$ axis and two parallel to the $-x$ axis, etc. They are activated in pairs to apply translational inputs and in opposed pairs to apply rotational commands. For the stuck-on thruster analysis, a single jet is assumed to fire continuously. All results will be given in terms of an inertial coordinate system that is defined to have origin at the initial position of the vehicle center of mass, $+x$ axis along the initial moment arm of the jet, and $+y$ axis along its initial thrust vector. Therefore, the resulting torque is along the $+z$, that is, positive yaw, axis. In addition, the amount of propellant that is consumed during the thruster firing is assumed to be sufficiently small that the resulting changes in vehicle mass properties are negligible. (This is certainly true for a vehicle such as AERCam Sprint, which has a total propellant capacity equal to less than 2% of its dry mass.)

Because a spherically symmetric body with a stuck-on thruster will experience rotation about a fixed axis, the planar thrust misalignment analysis of Ref. 9 can be used to describe its motion. In particular, the asymptotic Δv can be shown to be given as (formula 1, paragraph 3.691, Sec. 3.69–3.71, Ref. 10)

$$\Delta v_0 \approx \sqrt{I_0 \cdot \pi/2}\big/ m \cdot \sqrt{f/r} \tag{1}$$

where I_0 is the moment of inertia of this spherical vehicle about any axis. This velocity is made up of components of equal magnitude along the x and y axes. This expression certainly appears to be logical: If the jet moment arm is decreased or the inertia increased, the angular acceleration becomes smaller, thus, leading to a longer effective thrusting time before high rotation rates build up and, hence, to a greater final Δv. Similarly, increasing thrust or reducing vehicle mass gives a higher linear acceleration and, hence, a greater final velocity.

Figures 3 and 4, obtained for numerical values corresponding to an idealized spherical model for Sprint (Table 1), give more details of the resulting motion. Vehicle initial rates in both rotation and translation were taken to be zero, and orbital effects were neglected. Figure 3 shows the x, y, and z components of the linear velocity imparted to the vehicle over the first 50 s of the applied thrust; this

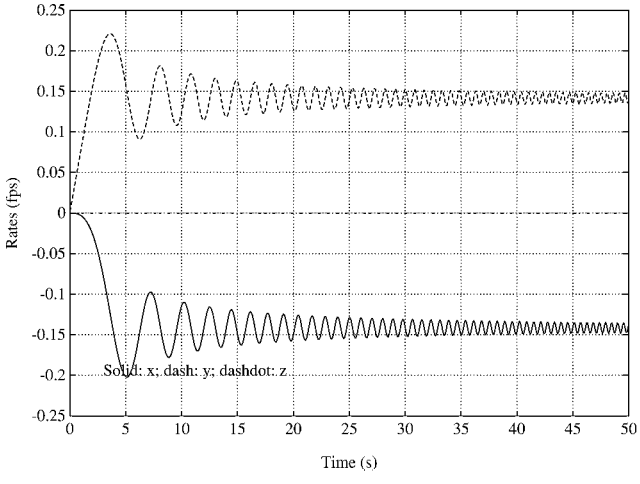

Fig. 3 Inertial linear rates, spherical model.

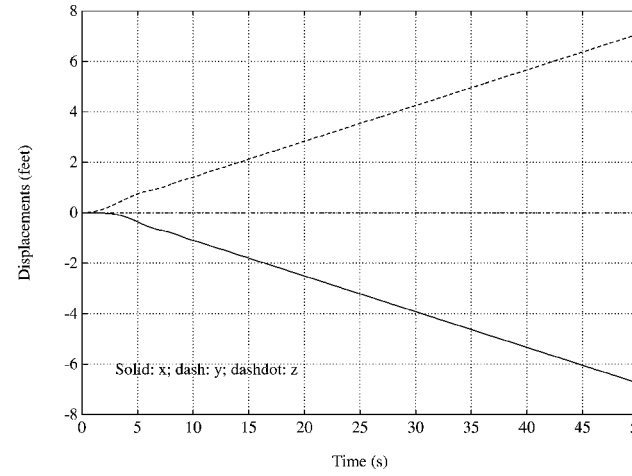

Fig. 4 Inertial linear displacements, spherical model.

behavior is analogous to that shown by Fig. 2 of Ref. 9. Figure 4 then gives the corresponding linear displacement components; this is analogous to the behavior shown in Fig. 3 of Ref. 9. Note that the z component in both Figs. 3 and 4 is zero: The vehicle executes a pure yaw rotation, so that the jet thrust vector remains in the xy plane throughout.

Note from Fig. 3 that the residual Δv that is applied to the vehicle by the stuck-on thruster is around 0.2 fps (0.06 m/s). This agrees with Eq. (1) for this vehicle. This speed is first achieved after about 2 or 3 s of thrusting. After that, the vehicle is continually rotating faster, so that the effect of any extra thrusting is merely to add a cyclic component, of monotonically decreasing amplitude and period, to the nonzero bias Δv_0. Thus, the body essentially travels away from the origin in a straight line at a steady rate (Fig. 4), with small superimposed oscillations. Because the final x and y components of velocity are of equal magnitude, the departure of the spacecraft is rotated through 45 deg from the initial direction of thrust of the stuck-on jet. Also, the time taken for the vehicle to rotate through 45 deg, 2.6 s, is about the same as that after which it has essentially achieved its final Δv. This suggests the following simplified method for calculating the residual Δv applied by a stuck-on thruster to a symmetric spacecraft: Until the vehicle has rotated through 45 deg, consider the applied thrust to be in the original jet direction; after this point, neglect the effect of further jet firing on linear motion. Note that the time taken to rotate through 45 deg, t_{45}, is given, in this single-axis rotation problem, by

$$t_{45} = \sqrt{\pi/2} \cdot \sqrt{1/\alpha_0} \tag{2}$$

where $\alpha_0 = rf/I_0$ is the angular acceleration of the vehicle in response to the stuck-on thruster. Writing the thrust/mass ratio for the jet as $a = f/m$, the resulting approximate Δv is then given as

$$\Delta v_0 \approx a t_{45} \tag{3}$$

Substituting for a and t_{45} in this expression can be seen to again yield Eq. (1). This confirms the validity of t_{45} as an approximate time constant for convergence to the final Δv for a spherically symmetric spacecraft with a stuck-on thruster.

Stuck-On Thruster, Near-Symmetric Case

The preceding analysis assumed a perfectly spherically symmetric vehicle. In practice, small asymmetries in the design of the spacecraft will be inevitable. In other words, the vehicle will have moments of inertia that are not exactly equal, small nonzero products of inertia, and perhaps some small nonzero offset between the vehicle center of mass and the geometric center of the thrusters. It will now be shown that prolonged firing of a jet on such a spacecraft can lead to a response that is markedly different, in its latter stages, from that obtained for the spherically symmetric case. In particular, the resulting net linear acceleration may be considerably greater than the ideal symmetric value. This long-term behavior is very important in

practice because thrusting that continues until propellant depletion or structural disintegration of the vehicle, whichever comes first, cannot be ruled out. (The Clementine mission experience[2] provides an illustration of the former.)

The response of a near-symmetric vehicle to a stuck-on thruster can be broken down into four main phases:

1) In the initial phase, the motion is quite similar to that encountered in the perfectly symmetric case.

2) In the transition phase, the motion becomes significantly different from that of the ideal vehicle. This phase is characterized by a rapid change in angular rates about all three axes and the start of an additional build up in linear Δv.

3) In the asymptotic phase, both linear Δv and angular rates increase approximately linearly with time. This phase continues until the thruster ceases firing.

4) The final phase is after thruster cutoff (if the vehicle remains intact).

Any real vehicle will inevitably possess some small amount of internal damping. Therefore, It is well known[11,12] that the coasting final phase will eventually develop into a spin about the major principal axis of the vehicle, that is that corresponding to the largest principal moment of inertia. Therefore, we shall concentrate only on the first three phases of the motion, where the addition of the constant thrusting term makes the resulting dynamic response different from the cases that are typically studied.

Initial/Transition Phases

Suppose the near-symmetric vehicle has center of mass location $\bar{\boldsymbol{x}}$ relative to the geometric center of its thrusters and inertia matrix $I = I_0 I_3 + \Delta I$ relative to its center of mass. In this expression, the scalar I_0 is the moment of inertia of the idealized symmetric vehicle about each axis, I_3 the (3×3) identity matrix, and the symmetric, generally fully populated, matrix ΔI satisfies $\|\Delta I\| \ll I_0$. The resulting jet torque is then

$$\boldsymbol{\tau} = (\boldsymbol{r} - \bar{\boldsymbol{x}}) \times \boldsymbol{f} = \boldsymbol{\tau}_0 - \bar{\boldsymbol{x}} \times \boldsymbol{f} \tag{4}$$

where $\boldsymbol{\tau}_0$ is the torque produced by this same thruster in the ideal case. Euler's equations then become

$$\boldsymbol{\tau} = I\dot{\boldsymbol{\omega}} + \boldsymbol{\omega} \times I\boldsymbol{\omega} = I\dot{\boldsymbol{\omega}} + \boldsymbol{\omega} \times \Delta I\boldsymbol{\omega} \tag{5}$$

making use of the fact that $\boldsymbol{\omega} \times I_0\boldsymbol{\omega} = \boldsymbol{0}$. To determine at what point the motion differs noticeably from the ideal case, define the relative rate

$$\delta\boldsymbol{\omega} = \boldsymbol{\omega} - \boldsymbol{\omega}_0 \tag{6}$$

where $\boldsymbol{\omega}_0(t)$ is the response in the ideal case. If we write similarly $\delta\boldsymbol{\tau} = \boldsymbol{\tau} - \boldsymbol{\tau}_0$, for $\boldsymbol{\tau}_0$ the torque in the spherical case, then Euler's equations reduce to

$$\begin{aligned}\boldsymbol{\tau}_0 + \delta\boldsymbol{\tau} &= (I_0 I_3 + \Delta I)(\dot{\boldsymbol{\omega}}_0 + \delta\dot{\boldsymbol{\omega}}) + (\boldsymbol{\omega}_0 + \delta\boldsymbol{\omega}) \times \Delta I\,(\boldsymbol{\omega}_0 + \delta\boldsymbol{\omega}) \\ &\approx (I_0\dot{\boldsymbol{\omega}}_0 + I_0\delta\dot{\boldsymbol{\omega}} + \Delta I\dot{\boldsymbol{\omega}}_0) + \boldsymbol{\omega}_0 \times \Delta I\boldsymbol{\omega}_0 \end{aligned} \tag{7}$$

omitting all terms of second or higher order in the perturbations ΔI and $\delta\boldsymbol{\omega}$. (This is somewhat analogous to the perturbation approach taken in Ref. 13 to simulate the motion of a body, with arbitrary moments of inertia, under the action of an external torque. However, the perturbations there were defined relative to the torque-free motion of the body; no mass property variations were considered.)

Also $\boldsymbol{\tau}_0 = I_0\dot{\boldsymbol{\omega}}_0$, so that we have $\delta\boldsymbol{\tau} \approx I_0\delta\dot{\boldsymbol{\omega}} + \Delta I\dot{\boldsymbol{\omega}}_0 + \boldsymbol{\omega}_0 \times \Delta I\boldsymbol{\omega}_0$, or

$$\delta\dot{\boldsymbol{\omega}} \approx \{\delta\boldsymbol{\tau} - \Delta I\dot{\boldsymbol{\omega}}_0 - \boldsymbol{\omega}_0 \times \Delta I\boldsymbol{\omega}_0\}/I_0 \tag{8}$$

For the particular thruster considered in the preceding section, we have

$$\boldsymbol{\tau} = \left\{ \begin{pmatrix} x_j \\ r \\ 0 \end{pmatrix} - \begin{pmatrix} \bar{x} \\ \bar{y} \\ \bar{z} \end{pmatrix} \right\} \times f \begin{pmatrix} 1 \\ 0 \\ 0 \end{pmatrix} = f \begin{pmatrix} 0 \\ -\bar{z} \\ -r + \bar{y} \end{pmatrix} = \boldsymbol{\tau}_0 + \delta\boldsymbol{\tau} \tag{9}$$

where $\boldsymbol{\tau}_0 = -rf\boldsymbol{e}_3$, $\delta\boldsymbol{\tau} = f(0\ -\bar{z}\ \bar{y})^T = fr(0\ -\tilde{z}\ \tilde{y})^T = \alpha_0 I_0 (0\ -\tilde{z}\ \tilde{y})^T$, and x_j is the (unimportant) x component of the jet position relative to the geometric center. Similarly, $\boldsymbol{\omega}_0(t) = -\alpha_0 t\boldsymbol{e}_3$ [$\boldsymbol{e}_3 = (0\ 0\ 1)^T$] is the ideal response in this case, with $\alpha_0 = rf/I_0$ the ideal angular acceleration. Equation (8) then becomes

$$\begin{aligned}\delta\dot{\boldsymbol{\omega}}(t) &\approx \left\{\delta\boldsymbol{\tau} + \alpha_0 \Delta I\boldsymbol{e}_3 - \alpha_0^2 t^2 \cdot \boldsymbol{e}_3 \times \Delta I\boldsymbol{e}_3\right\}\Big/ I_0 \\ &= I_0^{-1} \cdot \left\{ \delta\boldsymbol{\tau} + \alpha_0 \begin{pmatrix} \Delta I_{13} \\ \Delta I_{23} \\ \Delta I_{33} \end{pmatrix} - \alpha_0^2 t^2 \cdot \begin{pmatrix} -\Delta I_{23} \\ \Delta I_{13} \\ 0 \end{pmatrix} \right\} \end{aligned} \tag{10}$$

This expression can be simplified somewhat by defining the normalized change in inertia $\Delta\tilde{I} = \Delta I/I_0$ and center of mass shift $\tilde{\boldsymbol{x}} = \bar{\boldsymbol{x}}/r$. We then have

$$\delta\dot{\boldsymbol{\omega}}(t) \approx \alpha_0 \left\{ \begin{pmatrix} 0 \\ -\tilde{z} \\ \tilde{y} \end{pmatrix} + \begin{pmatrix} \Delta\tilde{I}_{13} \\ \Delta\tilde{I}_{23} \\ \Delta\tilde{I}_{33} \end{pmatrix} \right\} - \alpha_0^2 t^2 \cdot \begin{pmatrix} -\Delta\tilde{I}_{23} \\ \Delta\tilde{I}_{13} \\ 0 \end{pmatrix} \tag{11}$$

Integrating with respect to time then gives

$$\delta\boldsymbol{\omega}(t) \approx \alpha_0 t \left\{ \begin{pmatrix} 0 \\ -\tilde{z} \\ \tilde{y} \end{pmatrix} + \begin{pmatrix} \Delta\tilde{I}_{13} \\ \Delta\tilde{I}_{23} \\ \Delta\tilde{I}_{33} \end{pmatrix} \right\} - \frac{1}{3}\alpha_0^2 t^3 \cdot \begin{pmatrix} -\Delta\tilde{I}_{23} \\ \Delta\tilde{I}_{13} \\ 0 \end{pmatrix} \tag{12}$$

This first-order analysis shows that the deviation from the ideal angular acceleration is a small, roughly constant quantity for the initial phase of the motion. Dividing this constant deviation by the ideal acceleration α_0 gives a relative term that is of the same size as the normalized center of mass shift and normalized inertia variations. Note that the only inertia quantities that appear in Eq. (11) are the moment about the ideal spin axis and the products coupling this axis to the other two. The remaining inertias have only a negligible effect on the early motion of the vehicle and so do not play any role in this first-order analysis.

One further observation resulting from Eq. (12) allows a simple estimate of the time at which the transition phase of the motion begins. It can be seen that the term that is quadratic in time will first become significant when the time satisfies $\frac{1}{3}\alpha_0^2 t^3 = \alpha_0 t$. Therefore, this defines a time constant

$$t_{\text{trans}} = \sqrt{3/\alpha_0} \tag{13}$$

beyond which a linear analysis is no longer valid. For times greater than t_{trans}, the quadratic term in Eq. (11) and then the higher-order terms neglected in the derivation of this expression become increasingly large. These then give rise to the complicated dynamics expected in the transition phase. Therefore, this time constant is a good lower bound on the time at which transition begins. Note that t_{trans} depends only on the nominal angular acceleration of the ideal vehicle; it does not depend on the inertia variations or center of mass shift. [Of course, Eq. (11) shows that the constant difference between the angular accelerations in the real and spherical cases in the initial phase is proportional to these variations.] For the AERCam Sprint vehicle parameters given in Table 1, $\alpha_0 = 0.241\ \text{rad}/s^2$, giving a transition time constant of $t_{\text{trans}} \approx 3.5$ s. This agrees quite well with observed simulation results.

Asymptotic Phase

To study the fully developed asymptotic phase of the motion, it is more convenient to represent the dynamics of the vehicle in terms of its principal axes. In this coordinate system, the inertia perturbation matrix ΔI becomes diagonal and is denoted here by Λ. For simplicity, and without loss of generality, we shall shift the "nominal" inertia value I_0 so that all principal moment perturbations are either positive or zero, that is,

$$\Lambda = \begin{pmatrix} \lambda_1 & 0 & 0 \\ 0 & \lambda_2 & 0 \\ 0 & 0 & 0 \end{pmatrix} \tag{14}$$

with $\lambda_1 \geq \lambda_2 \geq 0$. In these coordinates, Euler's equations become

$$\hat{\tau} = (I_0 + \Lambda)\dot{\hat{\omega}} + \hat{\omega} \times \Lambda\hat{\omega} \tag{15}$$

where $\hat{\tau}$ and $\hat{\omega}$ are the applied torque and angular velocity, respectively, expressed in principal coordinates. As $\|I_0\| \gg \lambda_1$, we, therefore, have approximately that

$$I_0\dot{\hat{\omega}} = \hat{\tau} - \hat{\omega} \times \Lambda\hat{\omega} \tag{16}$$

When components are expanded, this reduces to the following three scalar Euler's equations:

$$\dot{\hat{\omega}}_1 = \{\hat{\tau}_1 + \lambda_2\hat{\omega}_2\hat{\omega}_3\}/I_0 \tag{17a}$$

$$\dot{\hat{\omega}}_2 = \{\hat{\tau}_2 - \lambda_1\hat{\omega}_3\hat{\omega}_1\}/I_0 \tag{17b}$$

$$\dot{\hat{\omega}}_3 = \{\hat{\tau}_3 + \Delta\lambda\hat{\omega}_1\hat{\omega}_2\}/I_0 \tag{17c}$$

where $\Delta\lambda = \lambda_1 - \lambda_2 \geq 0$.

The main question we wish to answer is how $\hat{\omega}$ evolves for large time values. The rate at which the magnitude of this vector grows will determine how long it will take the vehicle to reach a spin rate that will cause structural failure. Similarly, if the spacecraft is equipped with a centrifugal safety switch that deactivates the propulsion system once a certain spin rate is attained, knowledge of the asymptotic growth rate of $\hat{\omega}$ allows a prediction of the time that will be required before this switch trips. Knowledge of the asymptotic evolution of the direction of $\hat{\omega}$ allows a characterization of the inertial pointing of the jet thrust vector and, hence, calculation of the resulting Δv.

As a first step in this analysis, premultiply Eq. (16) by $\hat{\omega}^T$, giving

$$\hat{\omega}^T I_0\dot{\hat{\omega}} = \hat{\omega}^T\hat{\tau} - \hat{\omega}^T(\hat{\omega} \times \Lambda\hat{\omega}) = \hat{\omega}^T\hat{\tau} \tag{18}$$

Because I_0 is simply a scalar multiplier, the left-hand side of this equation is equal to $I_0\hat{\omega}^T\dot{\hat{\omega}}$. However, the identity $\boldsymbol{x}^T\boldsymbol{x} = x^2$, for any arbitrary vector $\boldsymbol{x}$ and its length x, can always be differentiated with respect to time to give $2\boldsymbol{x}^T\dot{\boldsymbol{x}} = 2x\dot{x}$. (Note that the scalar $\dot{x}$ is the rate of change of the length of $\boldsymbol{x}$, not the length of the vector $\dot{\boldsymbol{x}}$. Therefore, there is no implicit assumption here that the vectors $\boldsymbol{x}$ and $\dot{\boldsymbol{x}}$ are parallel.) Therefore, the left-hand side of Eq. (18) becomes (for $\boldsymbol{x} = \hat{\omega}$) $I_0\hat{\omega}\dot{\hat{\omega}}$, where $\hat{\omega}$ is the magnitude of $\hat{\omega}$, whereas the inner product on the right-hand side can be written as $\hat{\omega}\hat{\tau}\cos\theta$, where θ is the angle between $\hat{\omega}$ and $\hat{\tau}$. Therefore, rearranging gives

$$\dot{\hat{\omega}} = (\hat{\tau}/I_0) \cdot \cos\theta = \alpha_0\cos\theta \tag{19}$$

Thus, the rate at which $\hat{\omega}$ increases can never exceed α_0, the nominal angular acceleration of the ideal vehicle. In other words, $\hat{\omega}$ is a vector growing at most linearly with time. Suppose now that the direction of this vector does not coincide with any of the principal axes of the body. In this case, two or more of the (principal) components of $\hat{\omega}$ will be proportional to time. Let us say arbitrarily that these are components $\hat{\omega}_1$ and $\hat{\omega}_2$. Assuming that $\Delta\lambda > 0$, that is, $\lambda_1 > \lambda_2$, we then have from Eq. (17c) that $\dot{\hat{\omega}}_3$ is proportional to t^2 or that $\hat{\omega}_3$ varies as t^3, a contradiction. Therefore, for any body satisfying $\lambda_1 > \lambda_2 > 0$, only one of the components of $\hat{\omega}$ can increase linearly with time. In other words, $\hat{\omega}$ must asymptotically become aligned with one of the principal axes of the body.

Suppose first that $\hat{\omega}_2$ is the unbounded component of $\hat{\omega}$. Differentiating Eq. (17a) with respect to time then shows that

$$\begin{aligned}\ddot{\hat{\omega}}_1 &= \lambda_2[\hat{\omega}_2\dot{\hat{\omega}}_3 + \dot{\hat{\omega}}_2\hat{\omega}_3]/I_0 \\ &= \lambda_2[\hat{\omega}_2(\hat{\tau}_3 + \Delta\lambda\hat{\omega}_1\hat{\omega}_2) + (\hat{\tau}_2 - \lambda_1\hat{\omega}_3\hat{\omega}_1)\hat{\omega}_3]\big/I_0^2 \\ &\approx \hat{\omega}_1 \cdot \lambda_2\Delta\lambda\hat{\omega}_2^2\big/I_0^2\end{aligned} \tag{20}$$

because $|\hat{\omega}_2| \gg |\hat{\omega}_1|, |\hat{\omega}_3|$. However, λ_2 and $\Delta\lambda$ are positive whenever $\lambda_1 > \lambda_2 > 0$, and so this expression implies that $\hat{\omega}_1(t)$ will be divergent, another contradiction. Therefore, $\hat{\omega}$ cannot converge to the two-axis of the body, that is, that corresponding to its intermediate principal moment of inertia. This conclusion is very similar to the well-known one associated with torque-free motion of a rigid body.[4]

Therefore, convergence must be to either the major or minor principal axis of the body. Assume first that it is to the major axis in the case considered, that is, we have $|\hat{\omega}_1| \gg |\hat{\omega}_2|, |\hat{\omega}_3|$ for large enough values for time. It can then be shown, by a similar method to that used in Eq. (20), that the components of $\hat{\omega}$ about the other two axes satisfy

$$\ddot{\hat{\omega}}_2 \approx -\hat{\omega}_2 \cdot \lambda_1\Delta\lambda\hat{\omega}_1^2\big/I_0^2 \tag{21a}$$

$$\ddot{\hat{\omega}}_3 \approx -\hat{\omega}_3 \cdot \lambda_1\Delta\lambda\hat{\omega}_1^2\big/I_0^2 \tag{21b}$$

To simplify the notation, define the normalized inertia perturbations

$$\tilde{\lambda}_1 = \lambda_1/I_0, \qquad \tilde{\lambda}_2 = \lambda_2/I_0, \qquad \Delta\tilde{\lambda} = \Delta\lambda/I_0 \tag{22}$$

All of these quantities are much less than 1. Equations. (21) then become

$$\ddot{\hat{\omega}}_2 \approx -\hat{\omega}_2 \cdot \tilde{\lambda}_1\Delta\tilde{\lambda}\hat{\omega}_1^2, \qquad \ddot{\hat{\omega}}_3 \approx -\hat{\omega}_3 \cdot \tilde{\lambda}_1\Delta\tilde{\lambda}\hat{\omega}_1^2 \tag{23}$$

Therefore, the small components $\hat{\omega}_2(t)$ and $\hat{\omega}_3(t)$ are approximately sinusoidal, at frequency $\omega_{n1} = \hat{\omega}_1\sqrt{(\tilde{\lambda}_1\Delta\tilde{\lambda})}$. Hence, the term $\hat{\omega}_2\hat{\omega}_3$ on the right-hand side of Eq. (17a) is also cyclic, so that the mean value of $\hat{\omega}_1$ can be seen to be just $\hat{\tau}_1/I_0 \equiv \alpha_1$. [This is consistent with Eq. (19), because $\hat{\omega}_1 \approx \hat{\omega} = (\hat{\tau}/I_0) \cdot \cos\theta_1 = \alpha_1$, where θ_1 is the angle between $\boldsymbol{\tau}$ and the major principal axis. Note that the angular acceleration about the major axis during the initial, linear phase of the motion is also equal to α_1.] Therefore, the frequency of oscillation of the small components $\hat{\omega}_2(t)$ and $\hat{\omega}_3(t)$ is actually

$$\omega_{n1}(t) \approx \alpha_1\sqrt{\tilde{\lambda}_1\Delta\tilde{\lambda}} \cdot t \tag{24}$$

a quantity that increases linearly with time.

This motion admits quite a clear physical interpretation: It amounts to what can be termed forced nutation. In the case of standard torque-free nutation, the components of angular rate orthogonal to the spin axis describe a cone of fixed angle and rotate about it at constant rate. In the constant-thrusting case, on the other hand, the applied torque causes the rotation rate about the (principal) spin axis to increase roughly linearly with time. Therefore, the rate at which the vehicle nutates about this axis will also increase linearly with time. Similarly, the nutation angle will be reduced as the spin rate increases, giving approximate convergence to simple spin about this principal axis.

Very similar results apply if the vehicle converges to rotation about the minor principal axis, that is, if we have $|\hat{\omega}_3| \gg |\hat{\omega}_1|, |\hat{\omega}_2|$ asymptotically. The two small components again exhibit a form of modified simple harmonic motion. The frequency in this case is given as

$$\omega_{n3}(t) \approx \alpha_3\sqrt{\tilde{\lambda}_1\tilde{\lambda}_2} \cdot t \tag{25}$$

where $\alpha_3 = \hat{\tau}_3/I_0$.

It might be expected, in the light of the well-known instability of spins about the minor axis for a damped vehicle undergoing torque-free motion,[11,12] that convergence to a spin about the major axis is the only case that need be considered here. However, the fact that there is now an applied torque that can continuously put energy into the system leads to the result that minor axis convergence is indeed possible. Even if the vehicle possesses a small amount of internal damping, the energy input as a consequence of the work done by the applied torque will dominate the energy loss due to damping for any realistic damping model. A question that then arises is the following: In what circumstances will the vehicle converge to rotation about

the major axis, and when will it converge to a minor axis spin? This can be answered by examining the torque Rayleigh quotient

$$R(\boldsymbol{\tau}) = \frac{\boldsymbol{\tau}^T \Delta I \boldsymbol{\tau}}{\boldsymbol{\tau}^T \boldsymbol{\tau}} \tag{26}$$

This quantity always lies between 0 and λ_1, the minimum and maximum eigenvalues of ΔI. If $\lambda_1 > R(\boldsymbol{\tau}) > \lambda_2$, it can be shown that $\boldsymbol{\tau}$ lies in the region surrounding the major axis that is bounded by the separatrices[14] of this near-spherical body. Therefore, this torque will drive the angular velocity vector into this region also, that is, convergence will be to a major axis spin. On the other hand, if $\lambda_2 > R(\boldsymbol{\tau}) > 0$, then $\boldsymbol{\tau}$ lies in the region surrounding the minor axis. The vehicle will, therefore, asymptotically approach spin about the minor axis.

Note that this result is not equivalent to saying that convergence will be to that principal axis, major or minor, which is most closely aligned with the torque direction; the spread between the inertias of the vehicle also plays a very important role. In the extreme case of an exactly axisymmetric prolate vehicle with $\lambda_2 = \lambda_1 > 0$, it can be seen that convergence will be to the (minor) symmetry axis for any applied torque that is not precisely orthogonal to this symmetry axis. Similarly, an oblate axisymmetric vehicle with $\lambda_1 > \lambda_2 = 0$ will virtually always converge to the (major) symmetry axis. In more realistic cases where two of the principal moments are nearly, but not exactly, repeated, it can be seen that convergence will be to the axis corresponding to the isolated moment for almost all choices of torque vector.

This result has the following very important practical implication. For certain distributions of principal moments of inertia, the asymptotic rotation of the vehicle can be along a principal axis that is nearly orthogonal to the applied torque vector and, hence, may be roughly aligned with the direction of thrust of the stuck-on jet. Consequently, even though the vehicle is rotating at a high rate, there will be a relatively large component of linear acceleration that does not cancel over each cycle, namely,

$$a_1 = \boldsymbol{f}^T \boldsymbol{e}_1 / m \tag{27}$$

for asymptotic spin about the major axis (with unit vector $\boldsymbol{e}_1$) and

$$a_3 = \boldsymbol{f}^T \boldsymbol{e}_3 / m \tag{28}$$

for spin about the minor axis (unit vector $\boldsymbol{e}_3$). This is fundamentally different from what occurs in the initial phase of the motion, where rotation takes place about the direction of the applied torque, thus, giving rise to almost complete cancellation of the net applied force over each cycle. Furthermore, if the torque vector is nearly orthogonal to the asymptotic spin axis, the resulting angular acceleration about this axis, α_1 or α_3, has been shown to be quite low. Therefore, it would take a considerable time for any centrifugal safety cutoff switch on the vehicle to close, deactivating the propulsion system. Thus, not only is the asymptotic linear acceleration large in this case, but it may act for an extended period. The resulting net linear Δv can, therefore, be significant.

In the worst case, the net linear acceleration produced by the thruster in the asymptotic phase of the motion may approach the one-jet thrust/mass ratio, $a = f/m$, of the vehicle. In the best possible combination of thruster and principal axes, it may approach zero. However, this best case result applies only for one particular thruster, whereas it must be remembered that any one of the jets on the vehicle may stick on. Therefore, the quantity that should really be considered is the net linear acceleration $a_{\max}$ that will be obtained if the worst possible thruster fails on. It can be shown, by considering the direction cosines between the orthogonal principal axes of the body and the orthogonal thruster axes, that

$$a > a_{\max} \geq a/\sqrt{3} \tag{29}$$

As can be seen from the earlier discussion of the near-axisymmetric case, $a_{\max}$ will tend to be higher for such vehicles than for bodies with more widely spaced principal moments.

One final quantity that is of use in characterizing the motion is a measure of the time required for the vehicle to approach its asymptotic principal axis rotation. To this end, we define the time constant t_{asymp} to be that time at which the period of forced nutation, which asymptotically approaches zero, first becomes less than the elapsed time. Consider the major axis spin case first: This is equivalent to $2\pi/\omega_{n1}(t_{\text{asymp}}) = t_{\text{asymp}}$. From Eq. (24), this reduces to

$$t_{\text{asymp}} \approx \sqrt{\frac{2\pi}{\alpha_1 \sqrt{\tilde{\lambda}_1 \Delta\tilde{\lambda}}}} \tag{30}$$

The corresponding time constant for a minor axis spin is, from Eq. (25),

$$t_{\text{asymp}} \approx \sqrt{\frac{2\pi}{\alpha_3 \sqrt{\tilde{\lambda}_1 \tilde{\lambda}_2}}} \tag{31}$$

These expressions both reduce to just

$$t_{\text{asymp}} \approx \sqrt{2\pi/\alpha_a \tilde{\lambda}_1} \tag{32}$$

for the special case of an exactly axisymmetric vehicle, where α_a is the axial angular acceleration component. In fact, a simple lower bound in all cases is given by

$$t_{\text{asymp}} \geq \sqrt{2\pi/\alpha_0 \tilde{\lambda}_1} \tag{33}$$

Note that t_{asymp} is inversely proportional to the square root of the inertia perturbation magnitude $\|\Delta I\|$. Thus, the more perfectly symmetrical the vehicle is, the later the establishment of spin about a principal axis and, hence, the later the start of the undesirable large linear acceleration that may result. This contrasts with the time constant t_{trans} associated with the start of the transition phase, which was independent of $\|\Delta I\|$. In fact, the two time constants are related by

$$t_{\text{asymp}} \approx \sqrt{\frac{2\pi}{3\sqrt{\tilde{\lambda}_1 \Delta\tilde{\lambda}}}} \cdot \sqrt{\frac{\alpha_0}{\alpha_1}} \cdot t_{\text{trans}} \geq \sqrt{\frac{2\pi}{3\sqrt{\tilde{\lambda}_1 \Delta\tilde{\lambda}}}} \cdot t_{\text{trans}}$$

$$\geq \sqrt{\frac{2\pi}{3\tilde{\lambda}_1}} \cdot t_{\text{trans}} \tag{34}$$

for a major axis spin and very similar expressions for a minor axis spin. When the AERCam Sprint dynamic quantities given in Table 1 are used, and a maximum possible variation in the principal moments of inertia of 5% is assumed, Eq. (33) yields $t_{\text{asymp}} \geq 23$ s. As will be seen shortly, this agrees quite well with simulation results.

Finally, it can be seen from Eqs. (30–34) that minimizing the range of values of the principal moments of inertia of the body will, all else being equal, tend to delay the onset of asymptotic phase motion. Therefore, this will delay the point at which the vehicle may start to experience high linear accelerations. Furthermore, these inertias should, if possible, be evenly spaced. If, instead, two moments were much more closely spaced than the third, the body would be approximately axisymmetric. Hence, in light of the discussion following Eq. (26), high linear accelerations would be very likely to occur for many possible thruster orientations.

Summary of Stuck-On Thruster Response

The main relationships describing the response of a near spherically symmetric body to a stuck-on thruster can, therefore, be summarized as follows. In these results, $a = f/m$ is the one-jet thrust/mass ratio of the vehicle, $\alpha_0 = \tau/I_0$ is its ideal (spherical case) one-jet angular acceleration, $\{\alpha_i = \tau_i/I_0,\ i = 1, 2, 3\}$ are given from the principal components of the applied torque, λ_1 and λ_2 are the differences between the two larger actual principal moments of inertia and the smallest, $\{\tilde{\lambda}_i = \lambda_i/I_0\}$ are the normalized differences, and $\Delta\tilde{\lambda} = \tilde{\lambda}_1 - \tilde{\lambda}_2 \geq 0$.

The initial angular acceleration comprises components $\{\alpha_1, \alpha_2, \alpha_3\}$ along the principal axes of body.

The initial Δv applied (spherical body model) is $\Delta v_0 \approx a t_{45}$, where $t_{45} = \sqrt{[(\pi/2)/\alpha_0]}$.

The time constant of entry into transition phase is $t_{\text{trans}} = \sqrt{(3/\alpha_0)} (= 1.382 \times t_{45})$.

The principal axis converged to the major axis if $\lambda_1 > R(\tau) > \lambda_2$ and the minor axis if $\lambda_2 > R(\tau) > 0$, where the torque Rayleigh quotient $R(\tau) = \tau^T \Delta I \tau / \tau^T \tau$. If vehicle is exactly axisymmetric, convergence will almost always be to spin about the symmetry axis.

The time constant of entry into the asymptotic phase is $t_{\text{asymp}} \approx \sqrt{[2\pi/\alpha_1 \sqrt{(\tilde{\lambda}_1 \Delta\tilde{\lambda})}]}$ for major axis spin and $\sqrt{[2\pi/\alpha_3 \sqrt{(\tilde{\lambda}_1 \tilde{\lambda}_2)}]}$ for minor axis spin. In both cases, $t_{\text{asymp}} \geq \sqrt{(2\pi/\alpha_0 \tilde{\lambda}_1)} = \sqrt{(2\pi/3\tilde{\lambda}_1)} \cdot t_{\text{trans}}$.

The asymptotic angular acceleration is α_1 if along major axis and α_3 if along minor (as in initial phase).

The frequency of forced nutation is $\omega_{n1}(t) \approx \alpha_1 \sqrt{(\tilde{\lambda}_1 \Delta\tilde{\lambda})} \cdot t$ for spin about the major axis and $\omega_{n3}(t) \approx \alpha_3 \sqrt{(\tilde{\lambda}_1 \tilde{\lambda}_2)} \cdot t$ for minor axis spin.

The asymptotic linear acceleration is $a_1 = f^T e_1 / m$ for major axis spin and $a_3 = f^T e_3 / m$ for minor axis spin.

Simulation Results

The presented results will now be illustrated by simulation data. These will be obtained for two different near-symmetric spacecraft models based on the AERCam Sprint vehicle data given in Table 1. The spacecraft mass and nominal moments of inertia about each axis, together with the jet thrust magnitude and initial direction, thus, are the same values that were used to generate the results given earlier for the exactly symmetric case. In addition, principal inertia variations of up to 5%, representative[8] of a realistic vehicle, will now be included. The resulting inertia matrix, represented in the original body axes, will be diagonally dominant, with very small products of inertia. However, the associated principal axis directions can vary considerably, as a result of the extreme sensitivity of the principal axes of near-spherical bodies to minor mass asymmetries. For this reason, very different results can be obtained for inertia matrices that do not, on initial inspection, appear to differ significantly.

Example 1

The first near-symmetric configuration considered has inertia matrix

$$I_1 = \begin{pmatrix} 0.1656 & -0.0023 & 0.0016 \\ -0.0023 & 0.1658 & 0.0016 \\ 0.0016 & 0.0016 & 0.1614 \end{pmatrix} \text{kg} \cdot \text{m}^2 \qquad (35)$$

This corresponds to normalized moment of inertia variations of $\tilde{\lambda}_1 = 0.05$ and $\tilde{\lambda}_2 = 0.03$. Figure 5 shows the body rotation rates that result if the thruster that was considered in the symmetric case analysis again becomes stuck on. It can be seen that the motion does indeed begin by evolving linearly (for on the order of 5 s), but then moves on to the complicated transition phase. Figure 6 gives the corresponding rates about the principal axes. These rates exhibit the expected forced nutational behavior in the asymptotic phase (reached after around 25 s). Figure 6 shows that convergence is to a spin about axis 3, the minor axis. Note that the torque Rayleigh quotient of Eq. (26) can be shown to have value $R(\tau) = 0.0014 \text{ kg} \cdot \text{m}^2$ for this example; this is less than the (unnormalized) $\lambda_2 = 0.0048 \text{ kg} \cdot \text{m}^2$, so convergence is indeed predicted to be to a minor axis spin.

Figure 7 further illustrates the nature of this convergence showing the evolution with time of the angular velocity Rayleigh quotient $R(\omega) = \omega^T \Delta I \omega / \omega^T \omega$. [For initial time, this is approximately equal to $R(\tau)$ because the angular velocity is initially aligned with the torque.] The horizontal dashed lines in Fig. 7 denote the values of the eigenvalues of ΔI, that is, λ_1 (upper line), λ_2 (middle), and 0 (lower). Note that the $R(\omega)$ curve starts below the λ_2 line and remains below it throughout, with $R(\omega)$ asymptotically approaching the minor axis value of zero. This corresponds to convergence to a minor axis spin, in the manner described in the discussion following Eq. (26).

Figure 8 shows the resulting linear rates for this example, expressed in an inertial frame. Comparing Fig. 3 (ideal symmetric case) with Fig. 8 (near-symmetric case) reveals clearly the fundamental difference between these two cases, namely, the considerable translation rate that builds up along the z axis for the near-symmetric vehicle. It can be seen that the torque produced by the stuck-on thruster has the effect of reorienting the spacecraft so that the minor principal axis (the asymptotic spin axis) becomes oriented with the z axis (the initial spin axis). The component of jet thrust along the minor axis then leads to the asymptotic buildup in z-axis Δv. By the time the vehicle enters the asymptotic phase, this z-axis motion

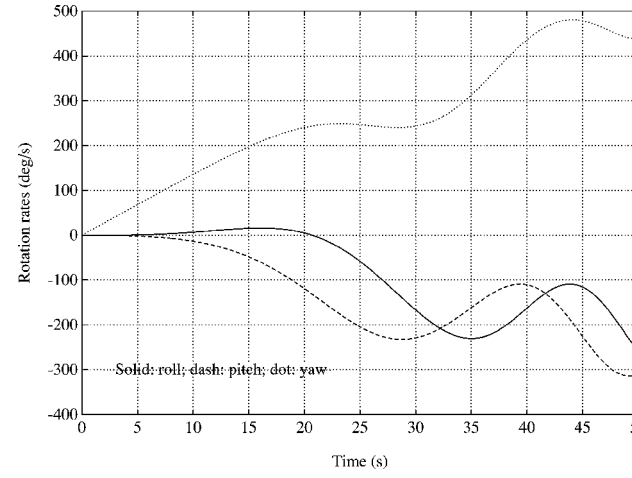

Fig. 5 Body axis rotation rates, example 1.

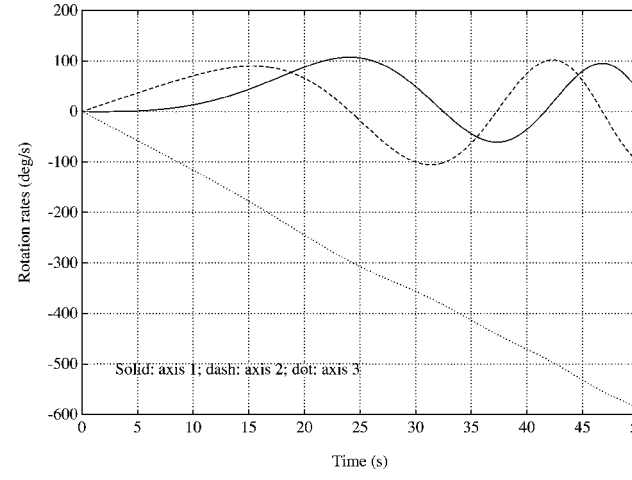

Fig. 6 Principal axis rotation rates, example 1.

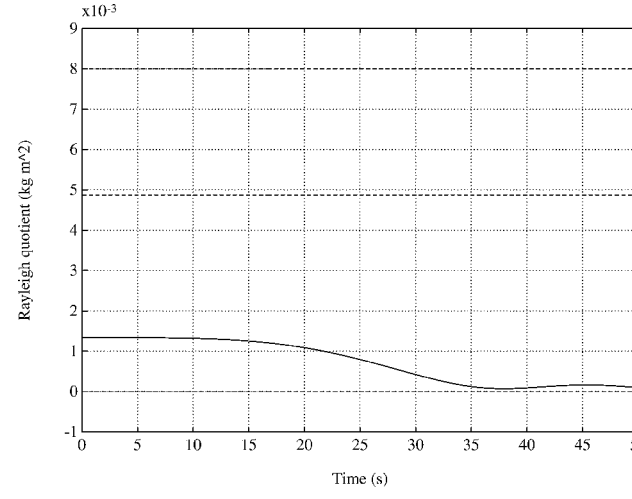

Fig. 7 Angular rate Rayleigh quotient, example 1.

Table 2 Dynamics parameters for example vehicles

Parameter	Example 1	Example 2
$\tilde{\lambda}_1$	0.05	0.05
$\tilde{\lambda}_2$	0.03	0.00
t_{45}, s	2.55	2.55
Δv_0, m/s	0.061	0.061
t_{trans}, s	3.53	3.53
Asymptotic spin axis	Minor	Major
t_{asymp}, s	28.4	40.5
a_{asymp}, m/s^2	0.009	0.023
α_{asymp}, rad/s^2	0.202	0.077
Nutation period, s	804/t	1640/t

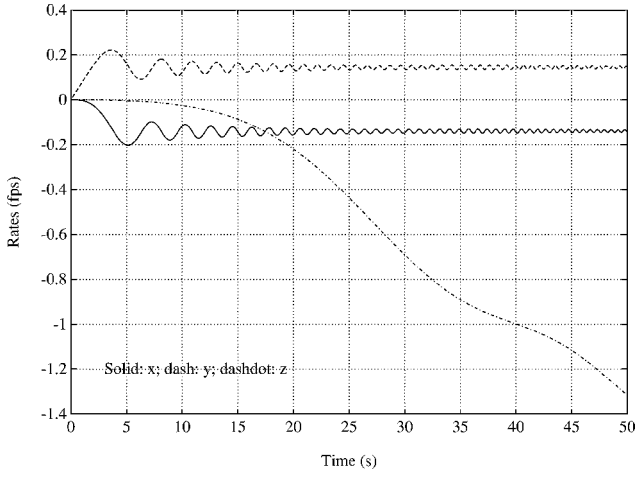

Fig. 8 Inertial linear rates, example 1.

dominates that along the other two axes. It is for this reason that an idealized symmetric model does not suffice for analysis of the behavior of a real near-spherical spacecraft under a stuck-on thruster: Such a model fails to capture the most significant long-term Δv source. In the current example, the angle between the thruster direction and the minor axis is 67.6 deg; therefore, the resulting asymptotic linear acceleration should be cos(67.6 deg) = 38% of the one-jet linear acceleration. This value of 0.009 m/s^2 (0.030 ft/s^2) agrees well with what is observed in the asymptotic phase of Fig. 8.

Finally, to compare more fully the new analytical stuck-on thruster expressions with the simulation results for this near-symmetric body, the second column of Table 2 lists the various analytical numerical values for this example system. It can be seen that the predicted time constants for entry into the transition and asymptotic phases, t_{trans} and t_{asymp}, respectively, agree closely with the approximate values of 5 and 25 s that were deduced from Figs. 5 and 6. Similarly, the asymptotic linear acceleration a_{asymp} and angular acceleration about the asymptotic spin axis α_{asymp} are also as observed from Figs. 8 and 6 (axis 3), respectively. Likewise, the frequency of forced nutation as predicted by Eq. (25) also agrees well with observations. This expression predicts a half-period of 10.9 s at an elapsed time of 37 s and 9.6 s at 42 s: These closely match the rotations about principal axes 2 and 1, respectively, that are seen in Fig. 6.

Example 2

Consider now a near spherically symmetric vehicle that is exactly axisymmetric oblate, with normalized inertia differences $\tilde{\lambda}_1 = 0.05$ and $\tilde{\lambda}_2 = 0$. The inertia matrix of this body is

$$I_2 = \begin{pmatrix} 0.1601 & -0.0007 & 0.0002 \\ -0.0007 & 0.1670 & -0.0025 \\ 0.0002 & -0.0025 & 0.1609 \end{pmatrix} \text{kg} \cdot \text{m}^2 \qquad (36)$$

If the same thruster as before becomes stuck on, the resulting rates about the principal axes are as given in Fig. 9; the corresponding

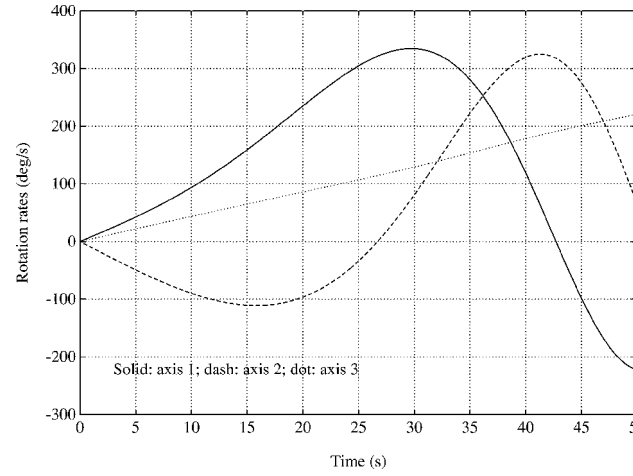

Fig. 9 Principal axis rotation rates, example 2.

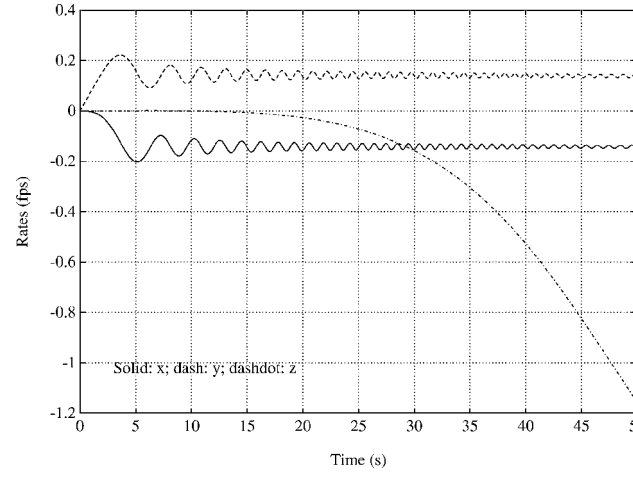

Fig. 10 Inertial linear rates, example 2.

linear rates are plotted in Fig. 10. Comparing Fig. 9 with Fig. 6 shows that the angular acceleration about the asymptotic spin axis for the second example is only about one-third as great as for the first. Conversely, comparing Figs. 8 and 10 reveals that the second system has an asymptotic linear acceleration value approximately double that of the first. Both of these observations are explained by the fact that Eq. (36) represents an axisymmetric body. As predicted following Eq. (26), the stuck-on thruster causes the vehicle to converge to spin about its symmetry, that is, major, axis, despite the fact that the applied torque is very nearly orthogonal to this axis. In fact, the angle between the torque direction and the symmetry axis is 70.4 deg for this example. This near orthogonality between torque vector and asymptotic spin axis gives rise to the low asymptotic angular acceleration of 0.077 rad/s^2 (4.4 deg/s^2) that is evident in Fig. 9. Similarly, the thrust vector is only 20.3 deg off the symmetry axis: Fig. 11 shows the approximate geometry, where the physical Sprintlike spacecraft is denoted by the solid sphere and its axisymmetric mass properties by the dashed oblate cylinder. That the angle between the thrust vector and the asymptotic spin axis is so small gives rise to a large thrust component along the spin axis and, hence, to the undesirably high linear acceleration of 0.023 m/s^2 (0.075 ft/s^2) that can be observed in the latter stages of Fig. 10. This value is equal to 94% of the one-jet thrust/mass ratio of the vehicle, confirming the prediction that a near spherically symmetric spacecraft with a stuck-on thruster can experience an acceleration that approaches this limit.

The predicted values given in Table 2 (third column) agree well with the observed simulation behavior for this example also. For instance, the increased value of t_{asymp} for example 2 is consistent with the somewhat slower entry into the full asymptotic phase that is

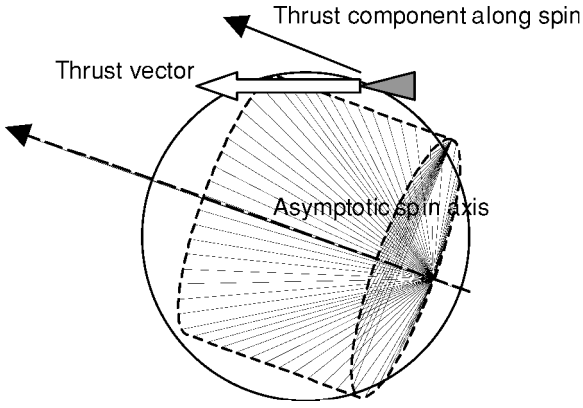

Fig. 11 Thruster and asymptotic spin geometry, example 2.

evident by comparing Figs. 8 and 10. Similarly, the asymptotic linear and angular accelerations discussed earlier are exactly as predicted. Finally, the analytical expression [Eq. (24)] for the frequency of forced nutation also gives values that agree with observations: The predicted half-periods of 28.2 s at an elapsed time of 29 s and 20.0 s at 41 s correspond closely to what is observed in Fig. 9 for rotation about axes 2 and 1, respectively.

Conclusions

The motion has been analyzed that is caused by a stuck-on thruster on a vehicle that is nearly spherically symmetric, as any real spacecraft that is intended to be perfectly symmetric will actually be. It was shown that the motion of such a vehicle is significantly more complicated than that which is obtained for the ideal case of a spherically symmetric body. In particular, the real spacecraft will experience a form of forced nutation, with convergence toward either its major or minor principal axis, depending on both the applied torque and the details of the mass properties of the vehicle. Furthermore, it was shown that this asymptotic spin axis need not be nearly orthogonal to the stuck-on thruster axis. Consequently, the body-fixed jet force vector may have a significant component along the spin axis, thus, giving rise to a considerable net linear acceleration of the spacecraft. The large Δv that can be produced in this way is not captured by an idealized, spherically symmetric model of the vehicle dynamics and can have important practical safety implications. For instance, it could lead to significant orbital perturbations and, in the case of proximity operations, a collision hazard. Furthermore, this large Δv will occur, to varying extents, for virtually all near-symmetric mass properties. Methods were derived for predicting this Δv, and other aspects of the stuck-on thruster behavior of near-symmetric vehicles, for any given set of mass properties, and the new analytical results that were derived were fully illustrated by means of numerical simulations.

Acknowledgments

This work was supported in part by the Automation, Robotics and Simulation Division at NASA Johnson Space Center under Grant NAG9-874, with Technical Monitor Keith Grimm.

References

[1] *Gemini Summary Conference*, NASA SP-138, 1967, pp. 52, 165.

[2] Hope, A. S., and Middour, J. W., "Clementine Mission Maneuver Performance and Navigation Control for the Spinning Phase," *Guidance and Control 1995*, Vol. 88, Univelt, San Diego, CA, 1995, pp. 463–476.

[3] Leimanis, E., *The General Problem of the Motion of Coupled Rigid Bodies about a Fixed Point*, Springer-Verlag, New York, 1965, pp. 136–178.

[4] Chobotov, V. A., *Spacecraft Attitude Dynamics and Control*, 1st ed., Krieger, Malabar, FL, 1991, pp. 26–29.

[5] Randall, L. A., Longuski, J. M., and Beck, R. A., "Complex Analytic Solutions for a Spinning Rigid Body Subject to Constant Transverse Torques," *Astrodynamics 1995*, Vol. 90, Pt. 1, Univelt, San Diego, CA, 1995, pp. 593–607.

[6] Tsiotras, P., and Longuski, J. M., "A Complex Analytic Solution for the Attitude Motion of a Near-Symmetric Rigid Body Under Body-Fixed Torques," *Celestial Mechanics and Dynamical Astronomy*, Vol. 51, No. 3, 1991, pp. 281–301.

[7] Livneh, R., and Wie, B., "New Results for an Asymmetric Rigid Body with Constant Body-Fixed Torques," *Journal of Guidance, Control, and Dynamics*, Vol. 20, No. 5, 1997, pp. 873–881.

[8] Williams, T. W., and Tanygin, S., "On-Orbit Engineering Tests of the AERCam Sprint Robotic Camera Vehicle," *Spaceflight Mechanics 1988*, Vol. 99, Univelt, San Diego, CA, 1998, pp. 1001–1020.

[9] de F. Rodrigues, D. L., and de O. e Souza, M. L., "Effects of Planar Thrust Misalignments on Rigid Body Motion," *Journal of Guidance, Control, and Dynamics*, Vol. 22, No. 6, 1999, pp. 916–918.

[10] Gradshteyn, I. S., and Ryzhik, I. M., *Table of Integrals, Series and Products*, Academic Press, New York, 1980, p. 395.

[11] Bracewell, R. N., and Garriott, O. K., "Rotation of Artificial Earth Satellites," *Nature*, Vol. 182, No. 4638, 1958, pp. 760–762.

[12] Wertz, J. R. (ed.), *Spacecraft Attitude Determination and Control*, Reidel, Dordrecht, The Netherlands, 1984, pp. 499–501.

[13] Kraige, L. G., "Perturbation Formulation for the Motion of an Arbitrarily Torqued Asymmetric Rigid Body," Ph.D. Dissertation, Dept. of Mechanical and Aerospace Engineering, Univ. of Virginia, Charlottesville, VA, May 1975.

[14] Kaplan, M. H., *Modern Spacecraft Dynamics and Control*, 1st ed., Wiley, New York, 1976, pp. 60, 61.

R. M. Cummings
Associate Editor